

Investigation of thermal resistance and power consumption in Ga-doped indium oxide (In₂O₃) nanowire phase change random access memory

Bo Jin, Taekyung Lim, Sanghyun Ju, Marat I. Latypov, Dong-Hai Pi, Hyoung Seop Kim, M. Meyyappan, and Jeong-Soo Lee

Citation: *Applied Physics Letters* **104**, 103510 (2014); doi: 10.1063/1.4868537

View online: <http://dx.doi.org/10.1063/1.4868537>

View Table of Contents: <http://scitation.aip.org/content/aip/journal/apl/104/10?ver=pdfcov>

Published by the AIP Publishing

Articles you may be interested in

[Investigation of electromigration in In₂Se₃ nanowire for phase change memory devices](#)

Appl. Phys. Lett. **103**, 233504 (2013); 10.1063/1.4838755

[Thermally efficient and highly scalable In₂Se₃ nanowire phase change memory](#)

J. Appl. Phys. **113**, 164303 (2013); 10.1063/1.4802672

[Dependence of the properties of phase change random access memory on nitrogen doping concentration in Ge₂Sb₂Te₅](#)

J. Appl. Phys. **107**, 104506 (2010); 10.1063/1.3383042

[Phase-change memory devices based on gallium-doped indium oxide](#)

Appl. Phys. Lett. **94**, 113503 (2009); 10.1063/1.3089238

[Indium selenide nanowire phase-change memory](#)

Appl. Phys. Lett. **91**, 133119 (2007); 10.1063/1.2793505

Want to publish your paper in the
#1 MOST CITED journal in applied physics?

With *Applied Physics Letters*, you can.

AIP | Applied Physics
Letters

THERE'S POWER IN NUMBERS. Reach the world with AIP Publishing.



Investigation of thermal resistance and power consumption in Ga-doped indium oxide (In_2O_3) nanowire phase change random access memory

Bo Jin,¹ Taekyung Lim,² Sanghyun Ju,² Marat I. Latypov,³ Dong-Hai Pi,³ Hyoung Seop Kim,³ M. Meyyappan,^{4,a)} and Jeong-Soo Lee^{1,a)}

¹Division of IT Convergence Engineering, Pohang University of Science and Technology (POSTECH), Pohang 790-784, South Korea

²Department of Physics, Kyonggi University, Suwon, Gyeonggi-Do 443-760, South Korea

³Department of Materials Science and Engineering, Pohang University of Science and Technology (POSTECH), Pohang 790-784, South Korea

⁴NASA Ames Research Center, Moffett Field, California 94035, USA

(Received 12 February 2014; accepted 2 March 2014; published online 14 March 2014)

The resistance stability and thermal resistance of phase change memory devices using ~ 40 nm diameter Ga-doped In_2O_3 nanowires (Ga: In_2O_3 NW) with different Ga-doping concentrations have been investigated. The estimated resistance stability ($R(t)/R_0$ ratio) improves with higher Ga concentration and is dependent on annealing temperature. The extracted thermal resistance (R_{th}) increases with higher Ga-concentration and thus the power consumption can be reduced by $\sim 90\%$ for the 11.5% Ga: In_2O_3 NW, compared to the 2.1% Ga: In_2O_3 NW. The excellent characteristics of Ga-doped In_2O_3 nanowire devices offer an avenue to develop low power and reliable phase change random access memory applications. © 2014 AIP Publishing LLC. [<http://dx.doi.org/10.1063/1.4868537>]

Phase change random access memory (PCRAM) has been widely investigated as a candidate for next generation nonvolatile memory.^{1,2} The phase change materials (PCMs) such as $\text{Ge}_2\text{Sb}_2\text{Te}_5$,^{3,4} GeSb ,⁵ and In_2Se_3 ⁶ have been characterized in terms of stability improvement, power reduction, and set/reset efficiency enhancement. Efforts to select a material with higher melting point or to add dopants in PCMs were attempted in order to improve the electrical stability.^{7,8} In recent years, the nanowire (NW) form of PCMs has been explored because the programming power can be effectively reduced due to the smaller active region and relatively lower melting point in nanoscale materials.^{5,9,10} The resistance stability and power consumption are critical for the reliability and multilevel capability of the device. Solutions to mitigate the resistance drift problem such as substitution of Ge by Sn,⁸ adding dopants to $\text{Ge}_2\text{Sb}_2\text{Te}_5$,¹¹ or scaling down the NW diameter¹² have been attempted.

More recently, the use of oxide-based NWs has been reported for PCRAM applications. Memory devices using Ga-doped In_2O_3 (Ga: In_2O_3) thin film have successfully shown repeatable switching behavior between crystalline and amorphous phases with a reduction in reset current for increased Ga doping.¹³ The Ga: In_2O_3 NW based PCRAM has also been reported wherein the operation voltage could be greatly reduced due to structural advantages and the electrical switching behavior was seen to depend on the Ga-concentration.¹⁴ Here, we report on the resistance stability ($R(t)/R_0$) and thermal resistance (R_{th}) related to power consumption of the Ga: In_2O_3 NW with three different compositions (Ga/(In + Ga) atomic ratio of 2.1%, 11.5%, and 13.0%). The Ga: In_2O_3 NW devices exhibit superior performance compared to other nanowires or thin films.

Single crystal Ga: In_2O_3 NWs were synthesized by vapor-liquid-solid (VLS) process in a horizontal tube furnace system. Three different amounts of Ga_2O_3 powder with molar ratio of 0.05%, 0.1%, and 0.5% mixed with 0.5 g InAs were individually placed in the source zone, and a SiO_2/Si substrate coated with ~ 20 nm Au particles was placed in the growth zone downstream from the source. The temperatures in the source and growth zones were maintained at 730°C and 650°C , respectively, for 60 min. PCRAM devices were fabricated by using the as-grown Ga: In_2O_3 NWs with three different compositions on a SiO_2 (300 nm)/Si substrate. 100 nm-thick indium-tin-oxide (ITO) as source and drain electrodes were deposited by using radio frequency sputtering system at room temperature and patterned by conventional photolithography. The NW channel regions were passivated with SiO_2 thin film (100 nm) in order to keep the NW surface from any reaction with the ambient air.

The as-grown Ga: In_2O_3 NWs were characterized by a high resolution field emission scanning electron microscope (HR FE-SEM, LEO SUPRA35) and a high resolution transmission electron microscope (HR-TEM, JEM-2100F) equipped with energy dispersive X-ray spectroscopy (EDS) for chemical composition analysis of individual NWs. The electrical characteristics of the devices were measured by a probe station Keithley 4200-SCS analyzer for current-voltage (I-V) and an Agilent 81110A voltage pulse-generator for set and reset operations, respectively. The external temperature was controlled by a ThermoChuck TPO3010 A/B.

Figure 1(a) shows FE-SEM images of the as-grown Ga: In_2O_3 NWs with a diameter of ~ 40 nm on a SiO_2 (300 nm)/Si substrate. All NWs with different Ga contents show the same morphology. The crystallinity of the nanowires was confirmed by the HR-TEM as in our previous study.¹⁴ Figure 1(b) shows HR-TEM image of a 11.5%

^{a)}Authors to whom correspondence should be addressed. Electronic addresses: m.meyyappan@nasa.gov and ljs6951@postech.ac.kr.

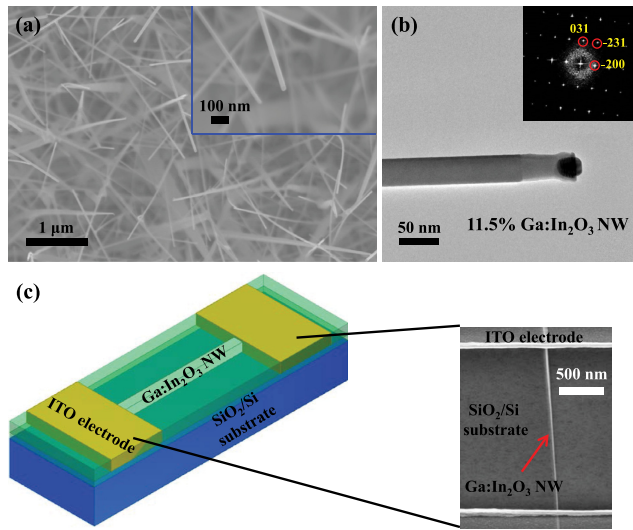


FIG. 1. (a) FE-SEM image of as-grown Ga:In₂O₃ NWs on a SiO₂/Si substrate. (b) HR-TEM image of an individual 11.5% Ga:In₂O₃ NW with ~40 nm in diameter. The right top inset represents diffraction pattern obtained by Fourier's transforming from an individual NW. (c) A schematic of Ga:In₂O₃ NW device and top view SEM image of the fabricated device with ~1.8 μm channel length between two ITO electrodes.

Ga:In₂O₃ NW with diffraction patterns obtained by Fourier transforming as shown in the inset. The stoichiometry of Ga and In of 1.0:46.7, 3.6:27.6, and 3.7:24.7 for the source composition has been obtained from the EDS analysis, and thus, the Ga/(In + Ga) atomic ratio is confirmed as 2.1%, 11.5%, and 13.0%, respectively.¹⁴ Figure 1(c) shows a schematic and a top view FE-SEM image of the fabricated device with a channel length of ~1.8 μm.

In PCRAM, the resistance in amorphous phase shows a steady increase during the elapsed time, a phenomenon known as resistance drift effect,¹⁵ which is described by a power law

$$\frac{R(t)}{R_0} = \left(\frac{t}{t_0}\right)^\alpha, \quad (1)$$

where t_0 is the initial time ($t_0 = 1$ s in this study), t is the elapsed time, R_0 is the initial resistance, $R(t)$ is the drifted resistance after time t , and α is the resistance drift coefficient. The measured $R(t)/R_0$ ratios for 2.1%, 11.5%, and 13.0% NW devices at room temperature are ~3, ~1.36, and ~1.2, respectively, as listed in Table I and shown in Figure 2(a). The ratio becomes smaller as Ga-concentration increases, which leads to lower resistance drift according to Eq. (1).

TABLE I. $R(t)/R_0$ Comparison of various Ga:In₂O₃ NW devices.

Ga-concentration (%)	Drift coefficient α	$R(t)/R_0$ ratio
2.1	0.134–0.186	~3
11.5	0.033–0.054	~1.36
13.0	0.016–0.042	~1.2

Figure 2(b) shows the resistance at reset state increasing with time for the 11.5% Ga:In₂O₃ NW device at 300 K and 375 K, respectively. The extracted drift coefficient α and $R(t)/R_0$ ratio were ~0.04 and ~1.36 at 300 K, and ~0.08 and ~1.78 at 375 K, respectively. Since α is proportional to the annealing temperature (T_A),^{15,16} the $R(t)/R_0$ ratio increases with annealing temperature.

Studies on the thermal resistance of the devices related to programming power consumption are critical for developing thermally efficient PCRAM devices. Considering that the reset operation of PCRAM is the power limiting step, the higher thermal resistance in crystalline phase can be effective for the reduction in reset power consumption. The relationship between the programming power and temperature in programming operation, derived from Fourier's equation, is given by

$$T_c = T_{300K} + R_{th} \times P_{prog}, \quad (2)$$

where T_c is the temperature of the active region in the NW device, T_{300K} is the room temperature 300 K, R_{th} is the thermal resistance, and P_{prog} is the electrical programming power. Crystallization occurs when the PCM is heated up to its crystallization temperature but below the melting point, whereas amorphization occurs when heated up to its melting point.^{17,18} Here, we assume T_c to be equal to 252 °C corresponding to the melting point of Ga:In₂O₃ material.¹³ From Eq. (2), the thermal resistance in crystalline phase was extracted as low as 1.64×10^5 K/W for 2.1% NW device and 2.22×10^6 K/W for 11.5% NW device, respectively, as shown in Figure 3(a). Compared to the ~1.37 mW reset power of 2.1% NW device, the 11.5% NW device exhibits 90% reduction in the reset power (~0.1 mW) due to its higher thermal resistance. In order to compare with the thin film devices, the P_{prog} , R_{th} , and other parameters are summarized in Table II. The 13.0% NW device is not considered because of its discontinuous switching behavior as in our previous work.¹⁴ The thermal resistance of NW devices is higher than that of thin film devices. Moreover, as shown in Figure 3(b), the higher Ga content can lead to higher thermal

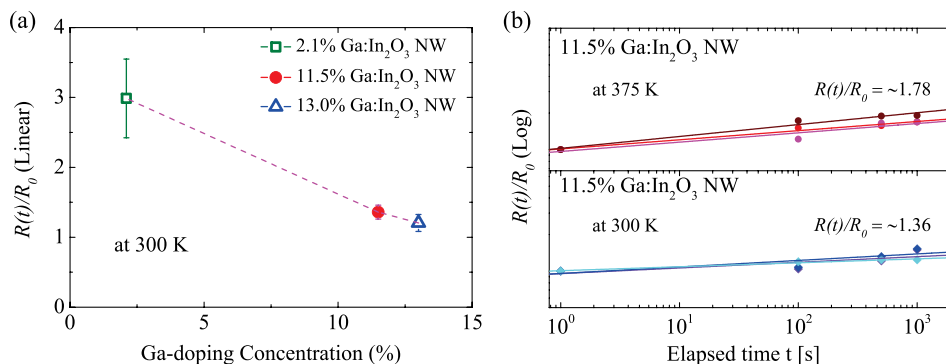


FIG. 2. (a) $R(t)/R_0$ ratio vs. Ga-doping concentration in Ga:In₂O₃ NW devices. (b) $R(t)/R_0$ ratio of 11.5% Ga:In₂O₃ NW devices at 300 K and 375 K, respectively.

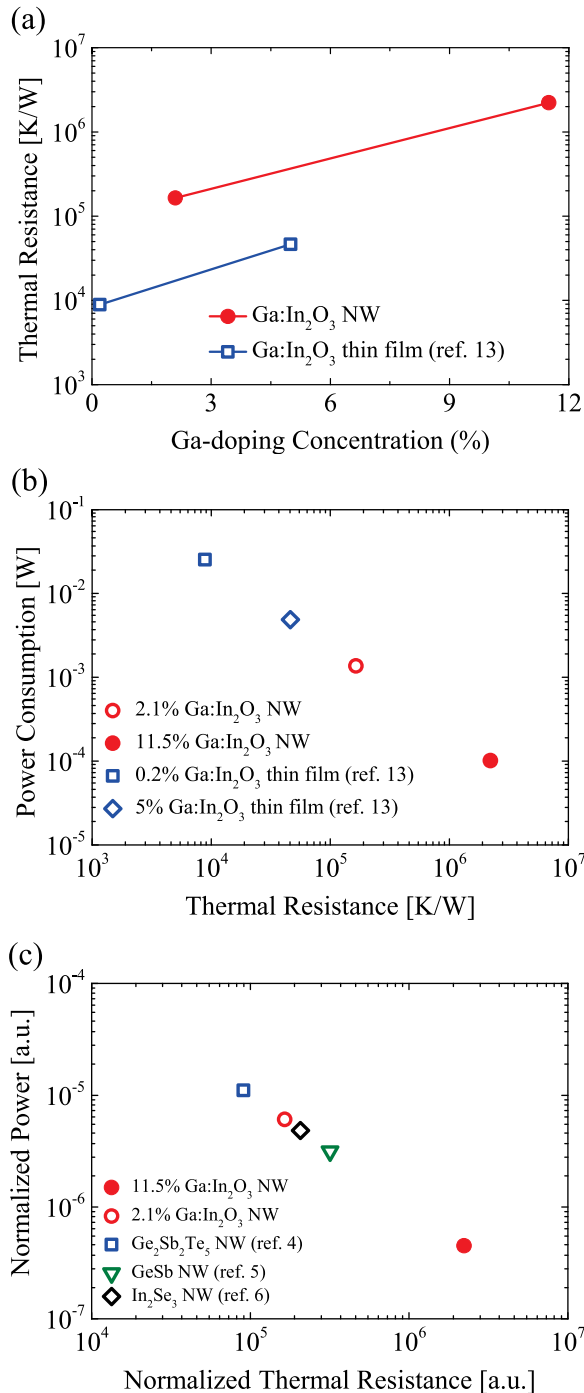


FIG. 3. (a) Ga-doping concentration dependent thermal resistance for Ga:In₂O₃ NW and thin film¹³ devices, respectively. (b) The higher thermal resistance of NW devices than that of thin film devices leads to a reduction in power consumption. The programming power for 11.5% NW device is as low as 0.1 mW for reset operation with the thermal resistance of 2.22×10^6 K/W. (c) 11.5% Ga:In₂O₃ NW has relatively higher thermal resistance than Ge₂Sb₂Te₅,⁴ GeSb,⁵ and In₂Se₃⁶ NWs, leading to lower power consumption.

resistance, and the increased thermal resistance can reduce the power consumption in reset operation.⁶ Figure 3(c) shows a relation between the P_{prog} and the R_{th} of Ga:In₂O₃ NW and other NW PCRAM devices. One can clearly observe that the 11.5% Ga:In₂O₃ NW device is relatively promising for low-power PCRAM applications compared to Ge₂Sb₂Te₅,⁴ GeTe,⁵ and In₂Se₃⁶ NW devices. Finally, pure indium and gallium oxide devices did not show any

TABLE II. Comparison of Ga:In₂O₃ NW and thin film^a devices on thermal resistance and power consumption.

Ga:In ₂ O ₃ device	Reset voltage V_{reset} (V)	Electrical resistance R (k Ω)	Power consumption P_{prog} (mW)	Thermal resistance R_{th} (MK/W)
2.1% NW	3.5	8.96	1.37	0.164
11.5% NW	3.0	88.7	0.1	2.22
0.2% thin film ^a	3.9	0.6	25.4	0.009
5% thin film ^a	5.4	6.0	4.86	0.046

^aSee Ref. 13.

switching behavior as they are not typical phase change materials. The phase change mechanism of Ga:In₂O₃ NWs will be investigated by *in-situ* TEM analysis in future work.

In summary, the thermal resistance and related power consumption of Ga:In₂O₃ NW PCRAM devices with different Ga compositions have been investigated. The NWs were synthesized by a VLS method, and two-terminal Ga:In₂O₃ NW devices were fabricated. The measured resistance stability ($R(t)/R_0$ ratio) shows dependence on Ga-concentration and annealing temperature with an improvement at higher Ga-concentration. The extracted thermal resistances are 0.164 MK/W for 2.1% Ga:In₂O₃ NW and 2.22 MK/W for 11.5% Ga:In₂O₃ NW, which are much higher than that of Ga:In₂O₃ thin film devices. Compared with other PCRAM NW devices, the 11.5% Ga:In₂O₃ NWs show more than one order of magnitude reduction in power consumption. The enhanced characteristics indicate that Ga-doped In₂O₃ NWs are promising for low power and reliable PCRAM applications.

This research was supported by National Research Foundation (NRF) (No. 2012R1A2A2A02010432); by the Basic Science Research Program (2011-0023219) through the Ministry of Science, ICT and Future Planning, Korea; and a grant (Code No. 2011-0031638) from the Center for Advanced Soft Electronics under the Global Frontier Research Program of the Ministry of Education, Science and Technology, Korea.

¹R. Bez and A. Pirovano, *Mater. Sci. Semicond. Proc.* **7**, 349 (2004).

²S. Raoux, R. M. Shelby, J. Jordan-Sweet, B. Munoz, M. Salinga, Y.-C. Chen, Y.-H. Shih, E.-K. Lai, and M.-H. Lee, *Microelectron. Eng.* **85**(12), 2330 (2008).

³S. H. Lee, Y. Jung, and R. Agarwal, *Nat. Nanotechnol.* **2**, 626 (2007).

⁴Y. Jung, S.-H. Lee, D.-K. Ko, and R. Agarwal, *J. Am. Chem. Soc.* **128**, 14026 (2006).

⁵X. H. Sun, B. Yu, G. Ng, M. Meyyappan, S. Ju, and D. B. Janes, *IEEE Trans. Electron Devices* **55**, 3131 (2008).

⁶B. Jin, D. Kang, J. S. Kim, M. Meyyappan, and J. S. Lee, *J. Appl. Phys.* **113**, 164303 (2013).

⁷D. B. Lee, S. S. Yim, H. K. Lyee, M. W. Kwon, D. M. Kang, H. G. Jun, S. W. Nam, and K. B. Kim, *Electrochem. Solid-State Lett.* **13**, K8 (2010).

⁸J. Luckas, A. Piarristeguy, G. Bruns, P. Jost, S. Grothe, R. M. Schmidt, C. Longeaud, and M. Wuttig, *J. Appl. Phys.* **113**, 023704 (2013).

⁹B. Yu, X. H. Sun, S. Ju, D. B. Janes, and M. Meyyappan, *IEEE Trans. Nanotechnol.* **7**, 496 (2008).

¹⁰A. N. Goldstein, C. M. Echer, and A. P. Alivisatos, *Science* **256**, 1425 (1992).

¹¹S. Song, Z. Song, L. Wu, B. Liu, and S. L. Feng, *J. Appl. Phys.* **109**, 034503 (2011).

¹²M. Mitra, Y. W. Jung, D. S. Gianola, and R. Agarwal, *Appl. Phys. Lett.* **96**, 222111 (2010).

- ¹³S. L. Wang, C. Y. Chen, M. K. Hsieh, W. C. Lee, A. H. Kung, and L. H. Peng, *Appl. Phys. Lett.* **94**, 113503 (2009).
- ¹⁴B. Jin, T. Y. Lim, S. Ju, M. I. Latypov, H. S. Kim, M. Meyyappan, and J. S. Lee, *Nanotechnology* **25**, 055205 (2014).
- ¹⁵I. V. Karpov, M. Mitra, D. Kau, G. Spadini, Y. A. Kryukov, and V. G. Karpov, *J. Appl. Phys.* **102**, 124503 (2007).
- ¹⁶S. B. Kim, B. Lee, M. Asheghi, F. Hurkx, J. P. Reifenberg, K. E. Goodson, and H. S. P. Wong, *IEEE Trans. Electron Devices* **58**, 584 (2011).
- ¹⁷B. Yu, S. Ju, X. H. Sun, G. Ng, T. D. Nguyen, M. Meyyappan, and D. B. Janes, *Appl. Phys. Lett.* **91**, 133119 (2007).
- ¹⁸Ph. Buffat and J. P. Borel, *Phys. Rev. A* **13**, 2287 (1976).